

Context-Based Meta Reinforcement Learning for Robust and Adaptable Peg-in-Hole Assembly Tasks

Ahmed Shokry^{1,2}

Shady A. Maged⁵

Walid Gomaa^{3,4}

Mohammed I. Awad⁵

Tobias Zaenker¹

Murad Dawood^{1,2}
Maren Bennewitz^{1,2}

Abstract—Peg-in-hole assembly in unknown environments is a challenging task due to onboard sensor errors, which result in uncertainty and variations in task parameters such as the hole position and orientation. Meta Reinforcement Learning (Meta RL) has been proposed to mitigate this problem as it learns how to quickly adapt to new tasks with different parameters. However, previous approaches either depend on a sample-inefficient procedure or human demonstrations to perform the task in the real world. Our work modifies the data used by the Meta RL agent and uses simple features that can be easily measured in the real world even with an uncalibrated camera. We further adapt the Meta RL agent to use data from a force/torque sensor, instead of the camera, to perform the assembly, using a small amount of training data. Finally, we propose a fine-tuning method that consistently and safely adapts to out-of-distribution tasks with parameters that differ by a factor of 10 from the training tasks. Our results demonstrate that the proposed data modification significantly enhances the training and adaptation efficiency and enables the agent to achieve 100% success in tasks with different hole positions and orientations. Experiments on a real robot confirm that both camera- and force/torque sensor-equipped agents achieve 100% success in tasks with unknown hole positions, matching their simulation performance and validating the approach’s robustness and applicability. Compared to the previous work with sample-inefficient adaptation, our proposed methods are 10 times more sample-efficient in the real-world tasks.

I. INTRODUCTION

Peg-in-hole (PiH) assembly tasks in unknown environments require the agent to rely on its onboard sensors to identify task parameters. Errors and noise in sensor readings significantly impact the estimated task parameters, such as hole position and orientation, which can lead to task failure. Previous work depends on vision sensors to estimate the approximate hole pose; then, model-based or learning-based methods are applied to compensate for the remaining errors in the estimated pose [1], [2]. Such model-based methods require prior knowledge about the environment and tuning effort by humans to work efficiently [3], [4].

Learning-based methods, such as RL, can autonomously learn to perform tasks without human intervention [5], [6]. However, they require a large amount of interaction data to learn the task and may exhibit unsafe exploration behavior

during training [7], [8]. That is why, Meta RL has been used since it learns how to quickly adapt to different tasks using the agent’s previous experience [9], [10]. The Meta RL agent is trained on multiple tasks and learns to adapt to each task using a limited amount of sampled data. During testing in a new task, the agent adapts by sampling data using the meta-trained policy, which avoids the unexpected exploration behavior in training from scratch and guarantees safety.

Meta RL has been used in PiH assembly to adapt to tasks with unknown hole positions [11], orientations, and peg shapes [12]. However, existing approaches either rely on a sensorless adaptation procedure [11], which lacks sufficient information about the new task and requires a large amount of sampled data to adapt, or depend on human demonstrations [12] to adapt to new tasks in the real world.

In this work, we propose to modify the data used by the agent to adapt to new tasks quickly. Instead of depending on human demonstrations [12] or information that cannot be precisely measured in the real world [11], we use data that can be accurately measured using detected hole features in 2D images without requiring accurate information about the camera calibration or the exact transformation matrix between the camera and the robot base frames. Fig. 1 shows an overview of our approach.

In addition to enhancing the real-world adaptation, the proposed modified data significantly improves the agent’s training efficiency by providing useful information about tasks. We further enhance the real-world applicability by adapting the meta-trained agent to use data from a force/torque sensor instead of the camera. The adaptation method requires significantly less data than that used during meta training. Finally, we propose a fine-tuning adaptation procedure that consistently and safely adapts the agent to out-of-distribution (OOD) tasks, which have different parameters, such as observations distribution, rewards, and dynamics, significantly differing from those of the training tasks. The contributions of our work are:

- 1) We modify the data used by the Meta RL agent, which enhances the training and adaptation efficiency of the agent and its real-world performance.
- 2) We introduce a sample-efficient procedure to adapt the Meta RL agent to use force/torque sensor data, which enhances the applicability of the agent in the real world.
- 3) We introduce a safe and consistent adaption procedure, which overcomes the limited generalization capabilities of Meta RL algorithms to out-of-distribution tasks.

¹Humanoid Robots Lab, University of Bonn and the Center for Robotics, Bonn, Germany. ²Lamar Institute for Machine Learning and Artificial Intelligence, Bonn, Germany. ³Cyber Physical Systems Lab, Egypt Japan University of Science and Technology, Alexandria, Egypt. ⁴Faculty of Engineering, Alexandria University, Alexandria, Egypt. ⁵Mechatronics Department, Ain Shams University, Cairo, Egypt.

This work has been supported by the BMBF within the Robotics Institute Germany, grant No. 16ME0999.

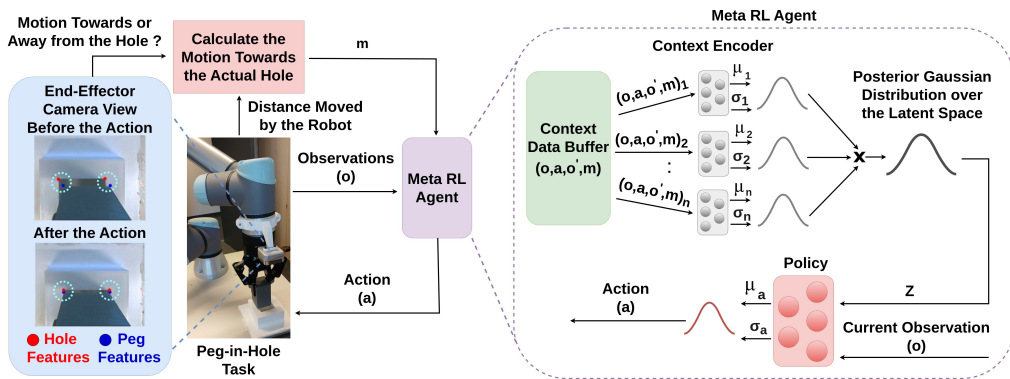


Fig. 1: The Meta RL agent depends on the robot observation o , which is the current peg position—calculated using the robot forward kinematics—in Cartesian coordinates, and the motion towards the actual hole m to implicitly infer the unknown hole position and perform the assembly task. m is calculated by adding the distances moved by the robot in each direction, the sign of each direction is positive if it results in reducing the distance between the detected hole and peg features in the 2D images captured before and after the motion by the end-effector camera, and negative otherwise. The context data consisting of the robot’s observations, next observations o' , m , and the agent’s actions a —representing the incremental distance to move the peg—is fed to the context encoder. This produces a posterior Gaussian distribution over the latent space, representing the agent’s belief about the current task. Latent variables sampled from this distribution are fed to the policy to adapt its behavior to the current task.

II. RELATED WORK

PiH assembly tasks have been extensively studied in the literature [1], [2], [13]. Hole search, i.e., estimating hole pose, is the most difficult and time consuming sub-task in PiH assembly [14]. Previous hole search methods can be categorized as heuristic-based methods, such as spiral and raster search [15], and sensor-based methods that use vision [16]–[18] and force/torque sensors [12], [19], [20] to estimate the hole pose and to successfully perform the assembly [2].

Heuristic-based methods are time-inefficient in case of considerable error in the estimated hole position and require tuning effort [14], [18]. Vision sensors are commonly used to estimate the hole pose, but they require precise calibration and an additional search step to compensate for the remaining error [18], [21]–[24]. Although previous work has achieved high accuracy in detecting hole features in 2D images, the error in the 3D or 6D pose arises from uncertainty and error in the depth information which is greatly affected by the type of the used sensor and the material of the hole [25], [26]. That is why we adapt the Meta RL agent to rely on the detected hole features in the 2D image only without the need for depth information or camera calibration. Force/torque sensors [27]–[29] and tactile sensors [30], [31] have also been used to estimate the hole pose. However, they suffer from sim-to-real gap [32], [33], which limits their usage in learning-based methods. Therefore, we propose a sample-efficient method that adapts the Meta RL agent, trained in simulation to effectively utilize force/torque sensor data using a limited amount of real-world data.

RL has been proposed to learn the robot actions directly from raw camera observations [34]–[36], and Meta RL was used in [11], [12] to perform assembly tasks with uncertainty in the hole pose and different peg shapes. In [11], the Meta RL agent was trained in simulation on tasks with different hole positions, then it was tested in the real world on tasks

with unknown hole positions. The agent depends on a reward requiring the actual hole position to adapt to new tasks. Although the actual hole position is available in simulation during training, it is not measurable during testing in the real world. As a result, the agent randomly explores the space of behaviors learned during meta training, which requires a large amount of interaction data and trials to adapt to the new task. In [12], the Meta RL agent was trained to use human demonstrations, instead of the immeasurable reward, to quickly adapt to tasks with different hole poses and peg shapes. However, human demonstrations may not be always available. Therefore, we propose the usage of modified data by the Meta RL agent that can be easily measured in the real world with onboard sensors.

In [37], context-based Meta RL agent was adapted to use different data. The meta-trained context encoder, which uses privileged information about the task as input and outputs a deterministic latent variable, was replaced by a new encoder. The new encoder uses a sequence of 50 transitions as input and produces the same output as the meta-trained encoder. On the other hand, our meta-trained and new context encoders use single transitions, whose data may be similar across multiple tasks, as input and produce a Gaussian distribution over the latent space.

III. APPROACH

We use the context-based Meta RL algorithm, PEARL [9], to perform PiH assembly tasks with unknown hole positions. An overview of our approach is represented in Fig. 1. The Meta RL agent depends on the current peg position, estimated from the robot forward kinematics, and the motion towards the actual hole m , calculated using the robot motion and features detected by the end-effector camera, to implicitly infer the unknown actual hole position and produce an action a , which is the incremental motion of the peg.

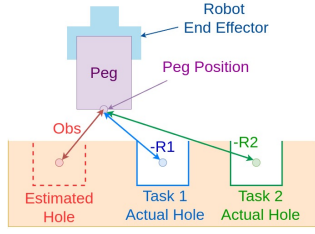


Fig. 2: The observation is the peg position relative to the estimated hole. The Reward is the negative L_2 distance between the peg and the actual hole position. Different actual hole positions have different rewards but the same observation.

A. Probabilistic Embeddings for Actor-Critic Reinforcement Learning (PEARL)

PEARL [9] is an off-policy, context-based Meta RL algorithm built on Soft Actor Critic (SAC) [7]. PEARL trains a context encoder that takes the context data $c = (o, a, o', r)$ as input, where o is the observation, o' the next observation, a the action, and r the reward. The output is a Gaussian distribution over a latent space representing the agent’s belief about the current task, where the variance explicitly represents the agent’s uncertainty. Latent variables sampled from this distribution are fed to the policy to adapt its behavior to the current task.

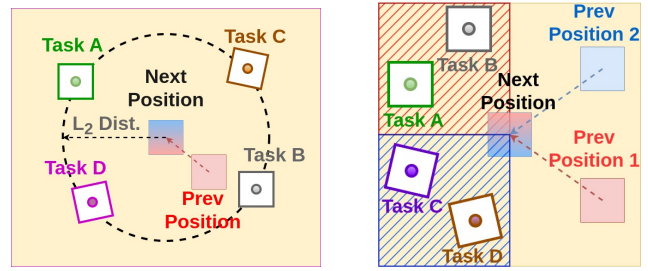
B. Environment Setup

We use the same environment setup as in [11], where the peg is grasped and the estimated hole position is available with an uncertainty of ± 4 mm, meaning that the actual hole can be up to 4 mm away from the estimated position in any horizontal direction. The hole clearance is 1 mm. The observation is defined as the peg position relative to the estimated hole, and the reward is the negative L_2 distance between the peg and the actual hole. As shown in Fig. 2, the actual hole can vary within the uncertainty region, resulting in different rewards, which is why each possible hole position is considered a separate task [11]. The action is defined as an incremental peg movement of up to 2 mm in each of the three Cartesian coordinates. The robot moves horizontally, then vertically, stopping when a high contact force is detected, followed by a small upward relieving motion, similar to the procedures used in [11], [16], [19].

As shown in Fig. 2, tasks share the same estimated hole position and observations, but have different rewards and dynamics inside the hole as the peg moves beneath the hole surface at a given position only if the actual hole is at that position; otherwise, collisions prevent downward motion.

C. Context Data Modification

Instead of using the negative L_2 distance reward as part of the context data as in [11], we use the motion towards the actual hole m , which is the summation of the distances moved by the robot in each Cartesian coordinate and the angle rotated around the vertical axis, in case of additional uncertainty in the hole orientation, due to the last action. The sign of each distance is positive if it is towards the actual hole



(a) Space of tasks with the same L_2 distance is represented by the black dashed circle. (b) Space of tasks with same motion towards the hole is represented by hashed squares.

Fig. 3: An example of tasks with the same (a) original and (b) modified context data for a given peg motion.

and negative otherwise. In the real world, the robot provides the value of each distance and the sign of the horizontal motions is determined by comparing the distances between the detected hole and peg features in the 2D images captured before and after the action as shown in Fig. 1. The sign of the vertical motion is determined based on the known hole height. However, it is mostly negligible outside the hole, as the peg moves very close to the hole surface.

The proposed modification also enhances the training and adaptation efficiency of the agent by providing more interpretable information about the task. Fig. 3a shows how for a given peg motion, tasks with the same L_2 distance from the peg may require completely opposite actions, which makes the agent uncertain about the suitable behavior and complicates the training and adaptation process. Conversely, tasks with the same motion towards the actual hole m for the same peg motion, represented by the red hashed square in Fig. 3b, require less different, and not opposite, actions. In case of additional uncertainty in the hole orientation, tasks with the same m may require opposite actions in one dimension only as represented by tasks C and D in Fig. 3b. However, it is still better than opposite actions in three dimension when using the L_2 distance as shown in Fig. 3a.

D. Adaptation to Different Sensor Data

We adapt the meta trained agent to use data from a force/torque sensor to perform the task by training an alterna-

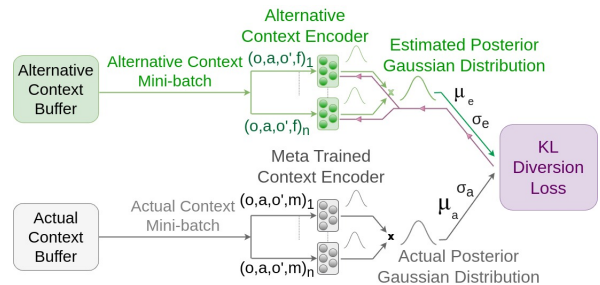


Fig. 4: Alternative encoder training. Random batches of actual and alternative context data are fed to the corresponding encoder and the KL-divergence between the actual and estimated posterior distributions is calculated. The KL-divergence loss is back-propagated (violet arrows) through the alternative context encoder to train and optimize it.

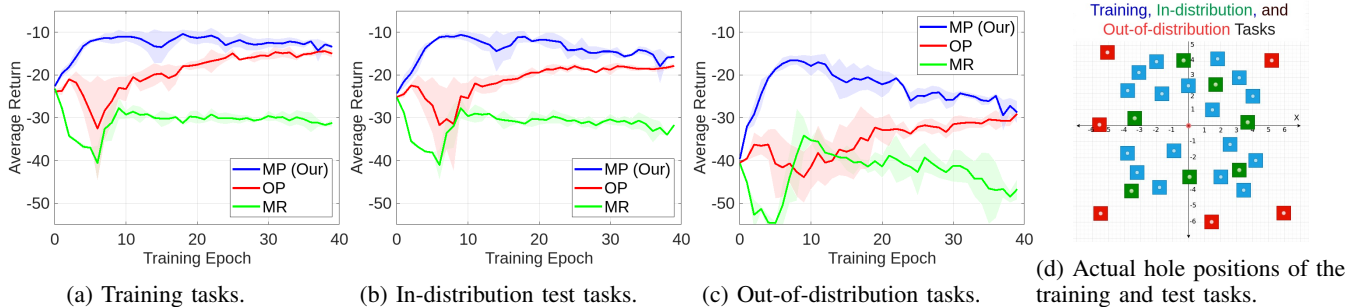


Fig. 5: The average returns of our modified PEARL (MP), the original PEARL (OP), and the PEARL with modified reward (MR) agents across the training epochs. As can be seen, our MP agent achieves the highest performance in all tasks compared to the other agents and it requires the least number of epochs to achieve its best performance. The actual position of all tasks relative to the estimated hole in millimeters is represented in (d).

tive context encoder using supervised learning. Our proposed adaptation method is shown in Fig. 4. First, the meta trained agent collects a limited amount of real-world data from different tasks with different actual hole positions using the prior normal distribution over the latent space. The collected actual context data (o, a, o', m) , with motion towards the actual hole m , and the alternative context data (o, a, o', f) , where f is the force/torque sensor readings, from each task are stored in separate buffers. Then, random batches are sampled from each task buffers and fed to the corresponding encoder. The outputs of each batch are multiplied to produce the actual and estimated posterior Gaussian distributions. The new alternative context encoder is trained to minimize the KL-divergence between the two posterior distributions.

Using the posterior Gaussian distributions for the loss calculation, rather than the output of each individual sample, enables the new encoder to assign different weights to the samples by assigning different variance. This approach is crucial because some data may be similar across multiple tasks, such as cases with no contact, or less informative about the task, such as cases with no overlapping between the peg and the hole. This data should be given less weight by assigning high output variance to it.

E. Out-of-Distribution Adaptation

As mentioned in Sec. III-B, our work considers tasks whose actual hole positions are within the range of 4mm around the estimated hole position. Tasks whose actual hole positions are located outside this range will be considered as out-of-distribution (OOD) tasks, which represent a challenge for context-based Meta RL [38], including PEARL [9].

We adapt to OOD tasks by, first, sampling exploration data using the normal prior distribution over the latent space and inferring the posterior distribution. this step leverages the agent’s previous experience to achieve the best possible initial behavior in OOD tasks. Then, we apply an iterative process of collecting exploration data using latent variables sampled from the current posterior distribution and optimizing the context encoder network to push the posterior distribution towards latent representations with high values of motion towards the actual hole m .

The context encoder is optimized to minimize the following loss:

$$L_{\text{OOD}} = -\alpha_1 \sum_{n=1}^N (\text{prob}(z_n) * m_n) + \alpha_2 \frac{1}{\sigma^2} + \alpha_3 (\mu - \overline{\mu}_i)^2 \quad (1)$$

where N is the number of data sampled using the current posterior distribution, m_n is the motion towards the actual hole using the latent variable z_n , μ and σ^2 are the mean and variance of the posterior Gaussian distribution produced by the context encoder outputs, $\overline{\mu}_i$ is the mean of the current posterior Gaussian distribution before optimization and the overline means stop gradient, α_1 , α_2 , and α_3 are tuning weights. The first term in Eq. 1 increases the probability of latent variables with high motion towards the actual hole and vice versa, using this term alone may severely decrease the variance which negatively affects the exploration in the subsequent steps. Therefore, we add the second term to penalize a small variance. The third term prevents huge changes in the posterior distribution between successive steps to ensure the safety and prevent any unpredictable behavior.

IV. EXPERIMENTS AND RESULTS

Our experiments are designed to prove the following:

- 1) The proposed context data modification enhances the training and adaptation efficiency of PEARL.
- 2) The proposed context data modification and the proposed method for different sensor adaptation enhance the real-world performance of the agent.
- 3) The proposed out-of-distribution adaptation method enables the agent to successfully and consistently adapt to tasks different from those of meta training.

Simulation experiments are conducted using MuJoCo [39], similar to [11], with a known actual hole position. Real-world tests use the UR5e robotic arm with a built-in force/torque sensor and the D405 RealSense camera mounted on the end-effector. We assume known peg features in the captured 2D images and hole features are detected using OpenCV [40] corner detection algorithm. Feature detection itself is not the main focus of this work since it is well studied in previous work. We mainly focus on the agent’s performance given the detected features in the 2D images. The Meta RL agent receives the current peg position from the robot and the

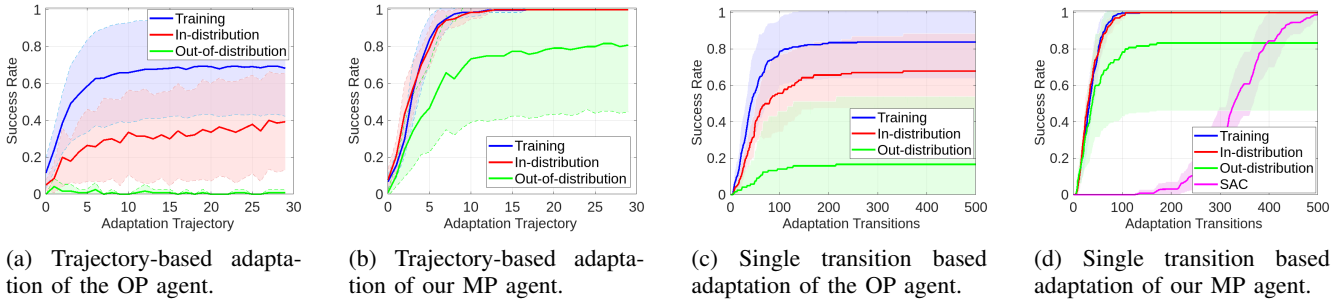


Fig. 6: Success rates of our modified PEARL (MP) (b,d) and the original PEARL (OP) (a,c) agents in simulation tasks. As can be seen, our MP agent outperforms the OP agent in all tasks and it is more sample-efficient than SAC.

estimated hole position to calculate observations, and outputs the incremental peg movement in Cartesian coordinates as action, which is converted into joint torque commands via MoveIt [41] and ROS (Robot Operating System) [42], as shown in Fig. 1. Both the policy and the context encoder are MLPs with three hidden layers of 200 neurons each. The latent variable has two dimensions in tasks with hole position uncertainty and five dimensions in case of additional uncertainty in the hole orientation.

A. Effect of the Proposed Context Data Modification

To evaluate the impact of the proposed context data modification, we trained two PEARL agents with identical architectures and hyper-parameters, differing only in their context data. The original PEARL (OP) [11] uses the context data $c = (o, a, o', r)$, where r is the negative L_2 distance reward, while our modified PEARL (MP) uses the context data $c = (o, a, o', m)$, where m is the motion towards the actual hole. Each agent is trained using three random seeds. The actual hole positions relative to the estimated hole position for training, in-distribution, and out-of-distribution test tasks are shown in Fig. 5d. In-distribution test tasks are new tasks within the same distribution of the training tasks.

1) *Training Efficiency*: We tested all agents after each epoch in all tasks for 10 trials, each consisting of 10 trajectories, and calculated the average return. Return is the summation of rewards across the trajectory. The average return of each agent’s random seeds across the training epochs is represented by solid lines in Fig. 5, while the shaded regions represent the standard deviation of the seeds returns. The results indicate that our MP agent achieves higher performance than the OP agent and it requires less number of epochs to achieve its best performance. This proves our claim that the modified context data provides better information and enhances the training efficiency.

The degradation of our MP agent performance, especially in test tasks in Fig. 5b and Fig. 5c, occurs because, as the agent’s performance improves, it samples more context data inside the hole, which is unique to each task (as detailed in Sec. III-B). The context encoder relies on this unique data to infer the task and gradually neglects the context data outside the hole, which is similar across multiple tasks as shown in Fig. 3b. This degrades the agent’s performance as it always starts outside the hole.

We trained a third agent (MR) that uses m as a reward,

instead of the negative L_2 distance, in addition to using it in the modified context data. The results in Fig. 5 show that using m as a reward degrades the agent’s performance, that is why our MP agent uses m in the context data only and uses the negative L_2 distance as a reward to train the agent.

2) *Adaptation Efficiency*: After meta training, the agents are tested in all tasks in simulation with a known actual hole position. The average success rate of each agent in each task type is represented by the solid lines in Fig. 6, while the shaded regions represent the standard deviation of the success rates in each task type. We adopt both trajectory-based adaptation, which updates the posterior distribution after each trajectory consisting of 50 steps [11], and single transition based adaptation, which updates the posterior distribution after each step. The success rate in each task is calculated based on 20 trials. The results show that our MP agent achieves a success rate of 100% in all the training and test tasks outperforming the OP agent. Even in OOD tasks, our MP agent is still able to achieve 80% success rate while the OP fails. Later, we will apply an adaptation procedure to enhance our MP agent’s performance in OOD tasks.

We additionally compare our MP agent with a single RL agent trained from scratch using SAC [7] and uses the motion m as a reward, because it is available to the agent during test time in the real world. We trained and tested the SAC agent in simulation to ensure safety. The results show that our MP agent is five times more sample-efficient than SAC.

3) *Robustness to more Sources of Uncertainty*: We adapted the agents to perform tasks with additional uncertainty in the hole orientation around the vertical axis. Success

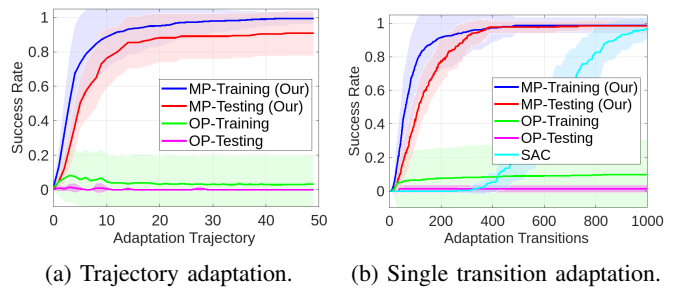


Fig. 7: Success rates of our modified PEARL (MP) agent and the original PEARL (OP) agent in tasks with uncertainty in the hole position and orientation. As can be seen, our MP agent significantly outperforms the OP agent in all tasks, and our MP agent is more sample-efficient than SAC.

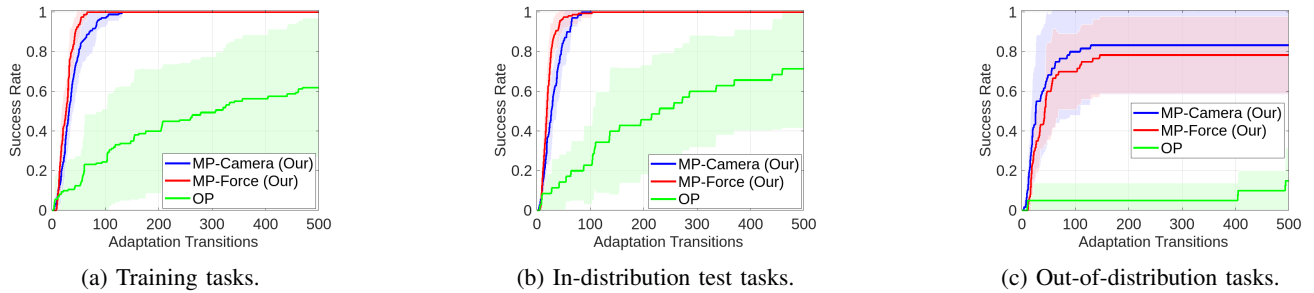


Fig. 8: Success rates of our modified PEARL agents using a camera (MP-Camera) and a force/torque sensor (MP-Force) and the original PEARL (OP) agents in the real world tasks. As can be seen, our MP agents outperform the OP agent.

rates of the OP and MP agents after training for 100 epochs are represented in Fig. 7. The OP agent fails to learn the task achieving only 10% success rate, while our MP agent achieves 100 % success rate in all tasks, except for 90% success rate in test tasks with trajectory-based adaptation. Similar to our previous results, our MP agent is more sample-efficient during adaptation than the SAC agent trained from scratch. These results prove the importance of our proposed context data modification and show that even if the actual hole pose is accurately known, the OP agent will not succeed.

B. Real-World Adaptation Performance

After meta training in simulation, we tested the OP and our MP agents in real-world assembly tasks with the actual hole offsets represented in Fig. 5d. The agents have information about the estimated hole position only with no information about the actual hole position. Additionally, we adapt our MP to use force/torque sensor data using the method proposed in Sec. III-D. The agent is adapted using 16,000 real-world samples, which is less than the data collected from one task per epoch during meta training, which is 32,000 samples.

Figure 8 shows the average success rate of our MP agent using the end-effector camera, as shown in Fig. 1, our MP agent using force/torque sensor data, and the OP agent using the sensorless trajectory-based adaptation procedure in [11]. The results show that our MP agents achieves 100% success rate in all the training and in-distribution test tasks within 100 adaptation steps. The OP agent achieves 70% success rate after 500 adaptation steps and shows inconsistent adaptation behavior as represented by the high standard deviation. The performance of our MP agent in the real world is nearly similar to its performance in simulation, shown in Fig. 6, which proves that our MP agent does not suffer from sim-to-real gap. The MP agent with force sensor achieves slightly faster adaptation because contact data is more informative about the hole position than m , which is similar across multiple tasks as shown in Fig. 3b. Compared to the results in the previous work [11], which requires 20 adaptation trajectories each consisting of 50 steps, i.e., 1,000 steps, to adapt to tasks with unknown hole position, our MP agents are 10 times more sample-efficient during real-world adaptation.

C. Out-of-Distribution Adaptation

We applied the adaptation procedure proposed in Sec. III-E to a number of challenging out-of-distribution

tasks whose actual hole offsets are in the range of 10, 20, 30, and 40 mm from the estimated hole position. The number of the transitions sampled per each posterior distribution N is 100 transitions. The success rate of the agent is represented in Fig. 9a. The results show that the agent is able to achieve 100% success in tasks with actual hole offsets which are 10 times greater than those used during meta training in 7,000 adaptation steps. Examples of the posterior distribution evolution in different tasks are shown in Fig. 9b, which show how the proposed method gradually, consistently, and safely explores the latent space.

V. CONCLUSION

Our work enhances previous methods that use PEARL [9] to perform peg-in-hole assembly tasks with unknown hole position by modifying the context data used by the agent to infer the current task and by training a new context encoder that can use different sensor data to perform the task. Our work solves multiple problems that face PEARL agent in assembly tasks, such as the immeasurable reward at test time, limited robustness to additional uncertainty in the hole orientation, and limited generalization to out-of-distribution tasks. Although our work focuses on peg-in-hole assembly tasks, the discussed problems and proposed methods are related to the PEARL Meta RL algorithm, and we claim that these methods can be beneficial for other tasks and applications.

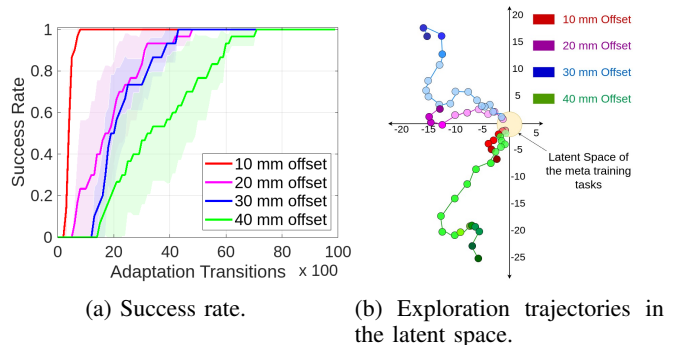


Fig. 9: Success rate of our proposed adaptation method in OOD tasks (a) and examples of the resulting exploration behavior in the latent space (b). As can be seen, our method consistently and gradually explores the latent space till success at tasks with 40 mm uncertainty in the hole position.

REFERENCES

- [1] J. Xu, Z. Hou, Z. Liu, and H. Qiao, "Compare contact model-based control and contact model-free learning: A survey of robotic peg-in-hole assembly strategies," *CoRR*, 2019.
- [2] Y. Jiang, Z. Huang, B. Yang, and W. Yang, "A review of robotic assembly strategies for the full operation procedure: Planning, execution and evaluation," *Robotics and Computer-Integrated Manufacturing*, 2022.
- [3] S. Chhatpar and M. Branicky, "Search strategies for peg-in-hole assemblies with position uncertainty," in *Proceedings 2001 IEEE/RSJ International Conference on Intelligent Robots and Systems.*, 2001.
- [4] J. A. Marvel, R. Bostelman, and J. Falco, "Multi-robot assembly strategies and metrics," *ACM Comput. Surv.*, 2018.
- [5] L. Stan, A. Nicolescu, and C. Pupaza, "Reinforcement learning for assembly robots: A review," *Proceedings in Manufacturing Systems*, 2020.
- [6] C. Tang, B. Abbatematteo, J. Hu, R. Chandra, R. Martín-Martín, and P. Stone, *Deep reinforcement learning for robotics: A survey of real-world successes*, 2024. arXiv: 2408.03539 [cs.RO]. [Online]. Available: <https://arxiv.org/abs/2408.03539>.
- [7] T. Haarnoja, A. Zhou, P. Abbeel, and S. Levine, "Soft actor-critic: Off-policy maximum entropy deep reinforcement learning with a stochastic actor," in *International conference on machine learning*, 2018.
- [8] L. Brunke, M. Greeff, A. W. Hall, *et al.*, "Safe learning in robotics: From learning-based control to safe reinforcement learning," *Annual Review of Control, Robotics, and Autonomous Systems*, 2022, ISSN: 2573-5144.
- [9] K. Rakelly, A. Zhou, C. Finn, S. Levine, and D. Quillen, "Efficient off-policy meta-reinforcement learning via probabilistic context variables," in *International conference on machine learning*, 2019.
- [10] C. Finn, P. Abbeel, and S. Levine, "Model-agnostic meta-learning for fast adaptation of deep networks," in *International conference on machine learning*, 2017.
- [11] G. Schoettler, A. Nair, J. A. Ojea, S. Levine, and E. Solowjow, "Meta-reinforcement learning for robotic industrial insertion tasks," in *Proc. of the IEEE/RSJ Intl. Conf. on Intelligent Robots and Systems (IROS)*, 2020.
- [12] T. Z. Zhao, J. Luo, O. Sushkov, *et al.*, "Offline meta-reinforcement learning for industrial insertion," in *2022 International Conference on Robotics and Automation (ICRA)*, 2022.
- [13] R. Li and H. Qiao, "A survey of methods and strategies for high-precision robotic grasping and assembly tasks—some new trends," *IEEE/ASME Transactions on Mechatronics*, 2019.
- [14] C. Wang, H. Luo, K. Zhang, H. Chen, J. Pan, and W. Zhang, "Pomdp-guided active force-based search for robotic insertion," in *Proc. of the IEEE/RSJ Intl. Conf. on Intelligent Robots and Systems (IROS)*, 2023.
- [15] J. Jiang, L. Yao, Z. Huang, G. Yu, L. Wang, and Z. Bi, "The state of the art of search strategies in robotic assembly," *Journal of Industrial Information Integration*, 2022.
- [16] A. Y. Yasutomi, H. Ichiwara, H. Ito, H. Mori, and T. Ogata, "Visual spatial attention and proprioceptive data-driven reinforcement learning for robust peg-in-hole task under variable conditions," *IEEE Robotics and Automation Letters*, 2023.
- [17] B.-S. Lu, T.-I. Chen, H.-Y. Lee, and W. H. Hsu, "Cfvs: Coarse-to-fine visual servoing for 6-dof object-agnostic peg-in-hole assembly," in *2023 IEEE International Conference on Robotics and Automation (ICRA)*, 2023.
- [18] R. Haugaard, J. Langaa, C. Sloth, and A. Buch, "Fast robust peg-in-hole insertion with continuous visual servoing," in *Proceedings of the 2020 Conference on Robot Learning*, 2021.
- [19] A. Yuji Yasutomi, H. Mori, and T. Ogata, "A peg-in-hole task strategy for holes in concrete," in *2021 IEEE International Conference on Robotics and Automation (ICRA)*, 2021.
- [20] H. Mao and J. Xiao, "Reducing uncertainty in pose estimation under complex contacts via force forecast," in *2020 IEEE International Conference on Robotics and Automation (ICRA)*, 2020.
- [21] L. Zheng, J. Ai, Y. Wang, *et al.*, "Deep visual-guided and deep reinforcement learning algorithm based for multip-peg-in-hole assembly task of power distribution live-line operation robot," *Journal of Intelligent and Robotic Systems*, 2024.
- [22] H. Kang, Y. Zang, X. Wang, and Y. Chen, "Uncertainty-driven spiral trajectory for robotic peg-in-hole assembly," *IEEE Robotics and Automation Letters*, 2022.
- [23] Y. Shen, Q. Jia, R. Wang, Z. Huang, and G. Chen, "Learning-based visual servoing for high-precision peg-in-hole assembly," *Actuators*, 2023.
- [24] K. Zhang, C. Wang, H. Chen, J. Pan, M. Y. Wang, and W. Zhang, "Vision-based six-dimensional peg-in-hole for practical connector insertion," in *2023 IEEE International Conference on Robotics and Automation (ICRA)*, 2023.
- [25] M. Servi, E. Mussi, A. Profili, *et al.*, "Metrological characterization and comparison of d415, d455, 1515 realsense devices in the close range," *Sensors*, 2021.
- [26] L. Burger, L. Sharan, R. Karl, *et al.*, "Comparative evaluation of three commercially available markerless depth sensors for close-range use in surgical simulation," *International journal of computer assisted radiology and surgery*, 2023.

- [27] L. Xie, H. Zhang, Y. Zhao, *et al.*, “Learning active force–torque based policy for sub-mm localization of unseen holes,” *IEEE Transactions on Industrial Informatics*, 2024.
- [28] S. Cao and J. Xiao, “A general method for autonomous assembly of arbitrary parts in the presence of uncertainty,” in *Proc. of the IEEE/RSJ Intl. Conf. on Intelligent Robots and Systems (IROS)*, 2022.
- [29] H. Mao and J. Xiao, “Reducing uncertainty in pose estimation under complex contacts via force forecast,” in *2020 IEEE International Conference on Robotics and Automation (ICRA)*, 2020.
- [30] S. Dong, D. K. Jha, D. Romeres, S. Kim, D. Nikovski, and A. Rodriguez, “Tactile-rl for insertion: Generalization to objects of unknown geometry,” in *2021 IEEE International Conference on Robotics and Automation (ICRA)*, 2021.
- [31] S. Kim and A. Rodriguez, “Active extrinsic contact sensing: Application to general peg-in-hole insertion,” in *2022 International Conference on Robotics and Automation (ICRA)*, 2022.
- [32] Y. Narang, K. Storey, I. Akinola, *et al.*, “Factory: Fast Contact for Robotic Assembly,” in *Proceedings of Robotics: Science and Systems*, 2022.
- [33] M. Noseworthy, B. Tang, B. Wen, *et al.*, “Forge: Force-guided exploration for robust contact-rich manipulation under uncertainty,” *arXiv preprint arXiv:2408.04587*, 2024.
- [34] A. Nair, B. Zhu, G. Narayanan, E. Solowjow, and S. Levine, “Learning on the job: Self-rewarding offline-to-online finetuning for industrial insertion of novel connectors from vision,” in *2023 IEEE International Conference on Robotics and Automation (ICRA)*, 2023, pp. 7154–7161. DOI: 10.1109/ICRA48891.2023.10161491.
- [35] G. Schoettler, A. Nair, J. Luo, *et al.*, “Deep reinforcement learning for industrial insertion tasks with visual inputs and natural rewards,” in *2020 IEEE/RSJ International Conference on Intelligent Robots and Systems (IROS)*, 2020, pp. 5548–5555. DOI: 10.1109/IROS45743.2020.9341714.
- [36] S. Levine, C. Finn, T. Darrell, and P. Abbeel, “End-to-end training of deep visuomotor policies,” *J. Mach. Learn. Res.*, 2016.
- [37] A. Kumar, Z. Fu, D. Pathak, and J. Malik, “Rma: Rapid motor adaptation for legged robots,” *Robotics: Science and Systems*, 2021.
- [38] J. Beck, R. Vuorio, E. Z. Liu, *et al.*, *A survey of meta-reinforcement learning*, 2024. arXiv: 2301.08028 [cs.LG]. [Online]. Available: <https://arxiv.org/abs/2301.08028>.
- [39] E. Todorov, T. Erez, and Y. Tassa, “Mujoco: A physics engine for model-based control,” in *2012 IEEE/RSJ International Conference on Intelligent Robots and Systems*, 2012.
- [40] Itseez, *Open source computer vision library*, <https://github.com/itseez/opencv>, 2015.
- [41] D. Coleman, I. A. Sucas, S. Chitta, and N. Correll, “Reducing the barrier to entry of complex robotic software: A moveit! case study,” *Journal of Software Engineering for Robotics*, vol. abs/1404.3785, 2014. [Online]. Available: <https://api.semanticscholar.org/CorpusID:13939653>.
- [42] M. Quigley, K. Conley, B. Gerkey, *et al.*, “Ros: An open-source robot operating system,” vol. 3, 2009.